

## A Novel Indium Doped Bismuth Nanofilm for Simultaneous Stripping Determination of Zn(II), Cd(II) and Pb(II) in River Water

Ruizhuo Ouyang<sup>\*</sup>, Lina Xu, Haifeng Wen, Penghui Cao, Pengpeng Jia, Tian Lei, Xia Zhou, Mei Tie, Xiaolei Fu, Yuefeng Zhao, Haizhou Chang, Yuqing Miao<sup>\*</sup>

University of Shanghai for Science and Technology, Shanghai 200093, China

<sup>\*</sup>E-mail: [ouyangrz@usst.edu.cn](mailto:ouyangrz@usst.edu.cn); [yqmiao@usst.edu.cn](mailto:yqmiao@usst.edu.cn)

Received: 11 September 2017 / Accepted: 19 November 2017 / Published: 28 December 2017

---

A novel indium doped bismuth hybrid nanofilm was prepared on a glassy carbon electrode (Bi@In/GCE) and successfully used for the simultaneous measurements of aqueous zinc (Zn(II)), cadmium (Cd(II)) and lead (Pb(II)). The Bi@In hybrid nanofilm was greatly improved in the ability of electron transfer, surface morphology as well as hydrophilicity over single Bi or In film, and exhibited well-defined and separate peaks for Zn(II), Cd(II) and Pb(II) by square wave stripping voltammetry. Analytical characteristics of the developed Bi@In/GCE were explored by comparing with single Bi and In film modified electrodes with calibration curves, which exhibited the most preferable electrochemical behaviors toward three metals as predicted. The synergistic effect of Bi and In mainly contributed to the enhanced electrochemical activity of the new electrode. In the concentration range of 0-120  $\mu\text{g L}^{-1}$ , a good linear relationship was achieved between the peak current and the metal concentration with correlation coefficient higher than 0.995. The detection limits were calculated to be 0.52, 0.15 and 0.67  $\mu\text{g L}^{-1}$  for Zn(II), Cd(II) and Pb(II) (S/N=3), respectively. The analysis of river sample with Bi@In/GCE was performed with satisfactory recoveries higher than 98%, suggesting that the new method is promising as a simple, sensitive and efficient approach to detect the heavy metals in water samples.

---

**Keywords:** Bi@In nanohybrid, Anodic stripping voltammetry, Cadmium, Zinc, Lead

### 1. INTRODUCTION

Heavy metal elements such as zinc (Zn(II)), cadmium (Cd(II)) and lead (Pb(II)) usually present in various matrices like environmental, food and biological samples due to continuous anthropic activities and are in return threatening human and environmental health because of their toxicity even in trace level[1, 2]. Quantifying concentrations of heavy metals in those matrices like river water,

biological fluids is of interest and significance because abnormal levels can cause both environmental pollutions and acute or chronic health problems[3-8]. Therefore, the determination of trace heavy metals in real samples has drawn considerable attention so far[4, 9-13]. It is of great importance to search for simple, rapid, sensitive and selective analytical methods to detect and monitor the level of heavy metal ions in real samples. Several atomic analysis spectroscopy techniques like atomic absorption spectrometry[14, 15], inductively coupled plasma atomic emission spectrometry[16] and inductively coupled plasma mass spectrometry[17] are usually used to determine trace heavy metals with sufficient sensitivity for most applications. However, the characters of high cost and time-consuming have made these methods less popular and attractive than electrochemical methods, especially electrochemical stripping analysis[1].

Electrochemical stripping techniques are particularly suitable for the determination of trace heavy metal ions in real samples due to their excellent sensitivity, preferable detection limits, relatively low cost and desirable capacity to multi-element determination [1, 3, 6, 9, 18, 19]. Currently, the fact that peak overlapping of different metal ions may usually encounter with the close redox potentials and possible interference from the formation of intermetallic compounds[20] has been often reported during the simultaneous and selective electrochemical sensing of several coexisted target metal ions such as Zn(II), Cd(II), Pb(II), etc. in real samples [4, 11, 21, 22]. Square-wave anodic stripping voltammetry (SWASV) is commonly selected for metal detection due to its high sensitivity, selectivity and low detection limit, resulting from a pre-concentration step to effectively accumulate metal on the electrode surface[11, 23-25].

Mercury-based electrodes including mercury film electrodes (MFEs)[26-28] and hanging mercury drop electrodes[29, 30] have traditionally been used in simultaneous determination of heavy metal ions *via* electrochemical stripping techniques owing to their advantages of high sensitivity, reproducibility, surface purity, high hydrogen overpotential as well as possibility of amalgam formation[1]. However, the toxicity of mercury inevitably causes environmental and human health concerns and thus restricts the wide use of those mercury based electrodes[7]. The development of “green”, “sustainable” or “environmentally friendly” analytical procedures becomes an active and growing research field[4]. Numerous attempts have consequently been made to replace mercury electrodes with alternative electrode materials which possess good analytical performance and the abovementioned characteristics. The metallic bismuth-film electrode (BiFE) was originally introduced in the year 2000 by Wang et al. for anodic stripping measurements of heavy metals and extensively explored as an environmentally friendly alternative to the well-known mercury electrodes in the following decades due to its similar stripping behaviors to those of mercury electrodes and the environmentally friendly nature [31]. Bismuth-based electrodes with superior voltammetric performance have been widely used because of the ability of bismuth to form “fused” alloys with heavy metals, its insensitivity towards dissolved oxygen and very low toxicity [1]. Up to date, the research on bismuth-based electrodes mainly involves in BiFEs which are highly advantageous in selectivity and sensitivity for the electrochemical analysis of heavy metals[31-37]. The Bi film is commonly generated through electrodeposition on substrates including glassy carbon electrodes (GCEs)[31], carbon paste electrodes (CPEs) [38] and screen-printed carbon electrodes (SPCEs)[1]. However, BiFEs produced this way are not easy to obtain satisfactory morphologies and the inherent

disadvantages of CPEs and SPCEs such as low mechanical stability and poor reproducibility limit their practical applications in stripping measurement of heavy metals[5, 7]. The applicability of other supporting materials has been described including carbon fibres[39], carbon nanotubes[3], mesoporous carbon[40], et al. to overcome the above weakness. We previously reported two types of electrodes modified with a bismuth entrapped mesoporous carbon[40] and a new bimetallic Hg-Bi/single-walled carbon nanotubes (SWCNTs) composite[3] modified GCEs with superior electrochemical performances to BiFEs toward the anodic stripping assay of Zn(II), Cd(II) and Pb(II), but the toxicity of mercury still brings environmental problems and the reproducibility need to be improved as well. In order to explore new desirable bismuth-based electrode, an indium doped Bi nanohybrid (Bi@In) was developed here by *ex-situ* electrodeposition to simultaneously monitor the level of heavy metal ions Zn(II), Cd(II) and Pb(II) in river water *via* SWASV technique. To the best of our knowledge, rare work on the bimetallic Bi@In based electrode was reported to simultaneously detect heavy metals. In the present work, Bi@In nanohybrid was, for the first time, successfully prepared on a GCE and well characterized by contact angle, the atomic force microscopy (AFM), the scanning electron microscopy (SEM) as well as electrochemical measurements. As expected, the remarkable improvement of the proposed Bi@In based sensor in voltammetric behaviors were achieved toward the stripping measurements of trace aqueous Zn(II), Cd(II) and Pb(II). The analysis of river water based on this new sensor was carried out successfully with results further verifying the sensor's promising reliability and precision toward the real time Zn(II), Cd(II) and Pb(II) monitoring.

## 2. EXPERIMENTAL

### 2.1. Chemicals and apparatus

#### 2.1.1 Chemicals

Acetic acid (HAc, glacial, 99.5%), sodium acetate (NaAc, anhydrous), potassium chloride (KCl, 99.5%), potassium ferrocyanide ( $K_4[Fe(CN)_6]$ ), potassium ferricyanide ( $K_3[Fe(CN)_6]$ ), cadmium nitrate ( $Cd(NO_3)_2 \cdot 4H_2O$ ), zinc nitrate ( $Zn(NO_3)_2 \cdot 4H_2O$ ) lead nitrate ( $Pb(NO_3)_2$ ), indium nitrate ( $In(NO_3)_3 \cdot 4H_2O$ ) and bismuth standard solution ( $1000 \text{ mg L}^{-1}$ ) were purchased from Aladdin chemical company (China) and used as received. The buffer solution (pH 4.5) was prepared by mixing 0.1 M NaAc and 0.1 M HAc. The buffer solution (pH 6.0) contained 0.1 M KCl and 0.1 M NaAc/HAc. Zn(II), Cd(II) and Pb(II) standards with different concentrations were prepared by diluting the appropriate amount of stock solution in electrolytes. All chemicals used are of analytical grade and all aqueous solutions were prepared with ultrapure water ( $>18 \text{ M}\Omega$ ).

#### 2.1.2 Apparatus

All electrochemical measurements were performed using a CHI electrochemical workstation (630D, CH Instruments, Inc.). A three-electrode configuration consisted of a Bi@In nanohybrid

modified GCE, Hg/Hg<sub>2</sub>Cl<sub>2</sub>, and a platinum wire (CH Instruments, Inc.) as working, reference and counter electrodes, respectively. The morphologies of the prepared nanomaterials were examined with an S-4800 UHR FE-SEM scanning electron microscope and an atomic force microscope (AFM, Nanonavi E-Sweep). Surface elemental analysis was performed with a AXIS Ultra<sup>DLD</sup> X-ray photoelectron spectrometer. The static water contact angle was measured at 25°C by a contact angle meter (OCA15 pro) employing drops of pure deionized water.

## 2.2. Preparation of In@Bi nanohybrid film

A GCE (3 mm diameter, CH Inc.) was polished to a mirror like surface using a standard electrode polishing kit (CH Instruments) including a 1200 grit Carbimet disk, 1.0 and 0.3 μm alumina slurry on a nylon cloth, as well as 0.05 μm alumina slurry on a microcloth polishing pad. After successive sonications in deionized water, ethanol and deionized water, the electrode was immersed in 0.1 M NaAc/HAc (pH 4.5) buffer solution containing 18 mg L<sup>-1</sup> Bi(III) and 12 mg L<sup>-1</sup> In(II) (mass ratio of 6:4) ions. The *ex-situ* co-deposition of Bi and In was thus performed at -0.90 V for 125 s under stirring. After being carefully rinsed with deionized water, the obtained Bi@In/GCE was used for subsequent assays.

## 2.3. Sample preparation

River samples were collected in polypropylene bottles from the Huangpu River in Shanghai, China. Prior to analysis, the river samples from three locations of the river were mixed and acidified with 3% nitric acid. Afterwards, the samples were filtered and stored in a freezer. 0.1 M acetate buffer solution (pH 6.0) was prepared with the pretreated river water and used to determine Zn(II), Cd(II) and Pb(II). Standard solutions of 10 and 20 μg L<sup>-1</sup> Zn(II), Cd(II) and Pb(II) were added individually to river water.

## 2.4. Analytical procedure

Electrochemical impedance spectroscopic (EIS) measurements were run in a solution containing 5 mM Fe(CN)<sub>6</sub><sup>3-/4-</sup> and 0.1 M KCl with a disturbance potential of 5 mV and a frequency range from 1 MHz to 1 Hz. 10 mL standard solution was used for electrochemical stripping experiments. At a preconcentration potential of -1.35 V, the accumulation of three metals at Bi@In/GCE was carried out under stirring. The stripping measurements were subsequently performed in the quiescent solution by square wave voltammetry (SWV) in a potential sweep range of -0.4 ~ -1.3 V with frequency of 15 Hz, step potential of 4 mV and amplitude of 25 mV. The SWASV scan started right after the accumulation step without a quite standing gap between. High-speed stirring accompanied the accumulation but stopped during the stripping measurements. An electrochemical cleaning step was applied at -0.3 V in 0.1 M NaAc/HAc solution containing 0.1 M KCl for 60 s

between measurements to guarantee the efficient removal of remaining Zn(II), Cd(II) and Pb(II) from GCE surface.

### 3. RESULTS AND DISCUSSION

#### 3.1 Electrochemical stripping behaviors of different electrodes

As mentioned, the electrochemical stripping technique is usually one the most sensitive techniques for the analysis of trace metals, which includes two steps: metal preconcentration at a given potential and stripping detection of metals. Here, the anodic stripping signal was used to measure the concentrations of Zn(II), Cd(II) and Pb(II) in aqueous solutions. For the determination of  $100 \mu\text{g L}^{-1}$  Zn(II), Cd(II) and Pb(II), square wave voltammograms were recorded in 0.1 M NaAc/HAc buffer solution (pH 6.0) and the anodic stripping peaks of Zn(II), Cd(II) and Pb(II) were observed at c.a. 1.15, 0.82 and 0.58 V, respectively, (Fig. 1).

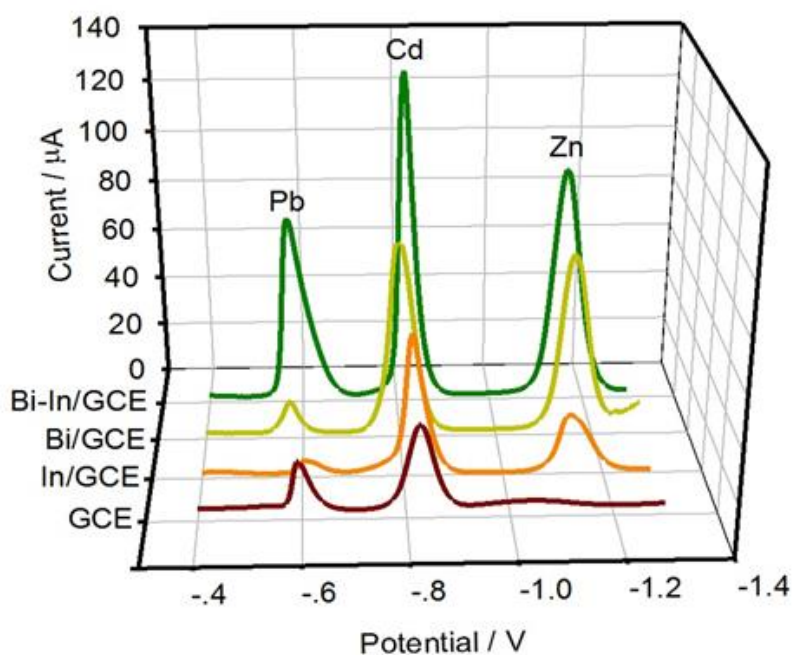


**Figure 1.** SWASV behaviors of bare GCE, Bi/GCE, In/GCE and Bi@In/GCE toward  $100 \mu\text{g L}^{-1}$  Zn(II), Cd(II) and Pb(II) in pH 6.0 solution containing 0.1 M NaAc/HAc and 0.1 M KCl.

Upon the comparison among bare GCE, Bi and In film modified GCE (Bi/GCE, In/GCE) as well as Bi@In/GCE, both Bi/GCE and In/GCE showed obviously higher stripping signals of Zn(II), Cd(II) and Pb(II) than bare GCE, indicating that either Bi or In film facilitated the stripping detection of the three metals. However, Bi@In/GCE exhibited the best stripping signals as-predicted. This means the presence of In within the Bi film could dramatically enhanced the stripping behavior of Bi@In/GCE. Conversely, the doped Bi improved the stripping performance of In/GCE toward the detection of three metals. In a word, the presence of either Bi or In exerted promotive effect to each other's electrochemical behavior due to the change of the electric double layer greatly depending on

the surface modification of electrode[6, 7]. The structure change in electric double layer may finally result in the activation energy change. As seen from Fig. 1, the Bi@In hybrid film remarkably decreased the activation energy of reaction occurring within the electric double layer and simultaneously accelerated the electrochemical reaction rate, which was verified by the fairly increased current signal of Bi@In/GCE over other three electrodes. The synergic effect of Bi@In nanohybrid was believed to make main contributions to the great improvements in anodic stripping performances of Bi@In/GCE toward Zn(II), Cd(II) and Pb(II).

### 3.2 Characterizations of Bi@In/GCE

#### 3.2.1 EIS characterization

EIS technique typically characterizes the electron transfer rate, an important role in the stripping detection of metals.

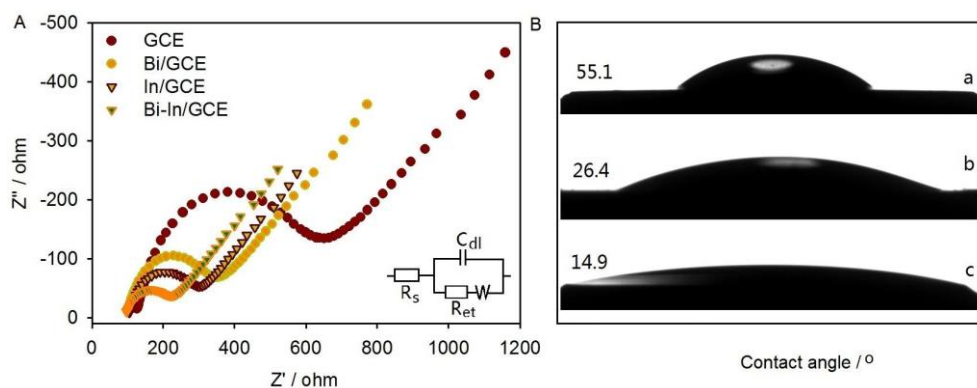


**Figure 2.** (A) EIS measurements of bare GCE, Bi/GCE, In/GCE and Bi@In/GCE in a solution containing 5 mM  $[\text{Fe}(\text{CN})_6]^{3-/4-}$  and 0.1 M KCl; (B) Contact angles of GCEs modified with Bi, In and Bi@In hybrid films.

Fig. 2A shows the Nyquist plots of bare GCE, Bi/GCE, In/GCE and Bi@In/GCE where the Randles circuit (*inset* of Fig. 2A) was introduced to fit the obtained impedance data. The electron-transfer resistance ( $R_{et}$ ) at the electrode surface is in a quite close relation with the semicircle diameter of Nyquist plot which reflects the double layer capacity ( $C_{dl}$ ) nature of the modified electrode. Without modification, the GCE showed the biggest semicircle among the four electrodes, revealing its poorest ability of electron transfer. Smaller semicircle diameter of Nyquist plot was found for both Bi/GCE and In/GCE, indicating that the electron transfer rate of GCE was improved by coating with either Bi or In film. However, a pretty small semicircle indicated the considerable impedance decrease of Bi@In/GCE surface, exhibiting the most favorable conductivity. The synergic effect and the good conductivity of Bi@In nanohybrid was likely responsible for the improvement in the stripping performance of Bi@In/GCE toward three metals.

### 3.2.2 Hydrophilicity study

The hydrophilicity of Bi/GCE, In/GCE as well as Bi@In/GCE was evaluated with contact angle (Fig. 2B). Poor hydrophilicity was observed for Bi/GCE with a contact angle of  $55.1^\circ$ . The smaller contact angle of  $26.4^\circ$  indicated the better hydrophilicity of In/GCE. However, a fairly low contact angle of  $14.9^\circ$  was observed for Bi@In/GCE, suggesting the excellent hydrophilicity of Bi@In/GCE. Good hydrophilicity is favorable for aqueous measurements, and Bi@In/GCE was accordingly used to detect aqueous Zn(II), Cd(II) and Pb(II).

### 3.2.3 Surface morphological study

The modifications of GCEs with Bi, In and Bi@In hybrid films were first studied through AFM measurements (Fig. 3). As shown, either Bi (Fig. 3A) or In (Fig. 3A) film exhibited a thin and smooth surface with the mean roughness of 3.1 and 2.9 nm, respectively.

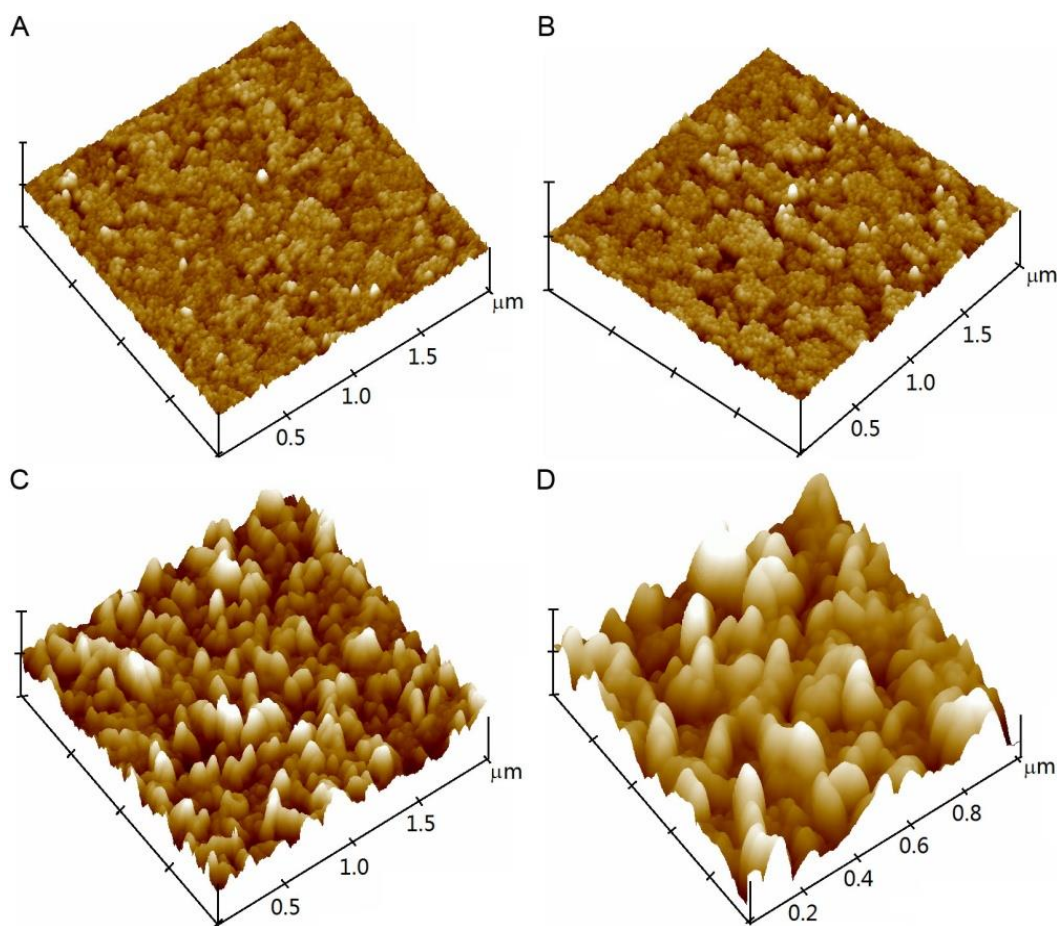


**Figure 3.** AFM images of GCEs modified with (A) Bi film, (B) In film and (C and D) Bi@In hybrid film.

By comparison, an apparently thicker and rougher surface formed after the co-deposition of Bi and In on GCE surface (Fig. 3C and D) with the mean roughness of 10.9 nm. To some extent, the

rougher the film is, the more active sites and surface area are available for metal detection. This could be one of the reasons that Bi@In/GCE showed the best stripping signal toward Zn(II), Cd(II) and Pb(II) over the other three electrodes mentioned above.

SEM images were obtained as well to further investigate the surfaces of electrodes modified with Bi, In and Bi@In films (Fig. 4). Similar to AFM images, either Bi or In film electrode showed a relatively smooth surface, which was made of many small particles. Like previously reported, the size of Bi particles was quite different [7]. Whereas, the co-deposition of Bi and In generated larger and more uniform hybrid particles on GCE surface, which was believed to have larger surface and more active sites exposed to Zn(II), Cd(II) and Pb(II) for stripping responses.

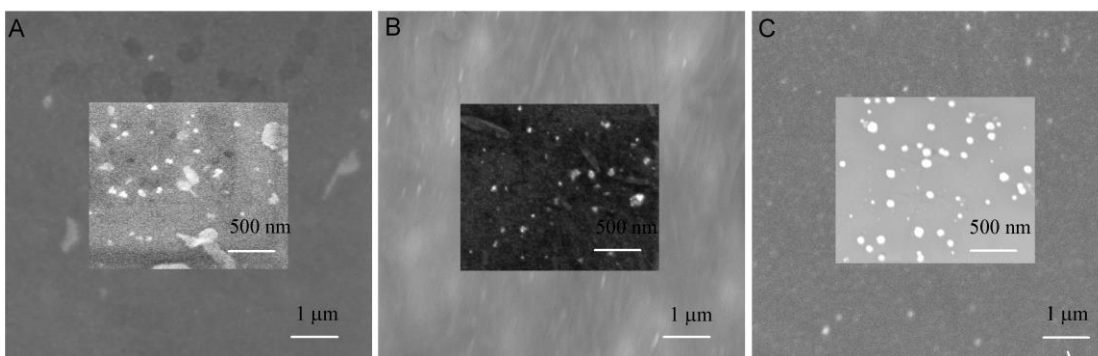


**Figure 4.** SEM images of Bi/GCE, In/GCE and Bi@In/GCE.

### 3.2.4 XPS analysis

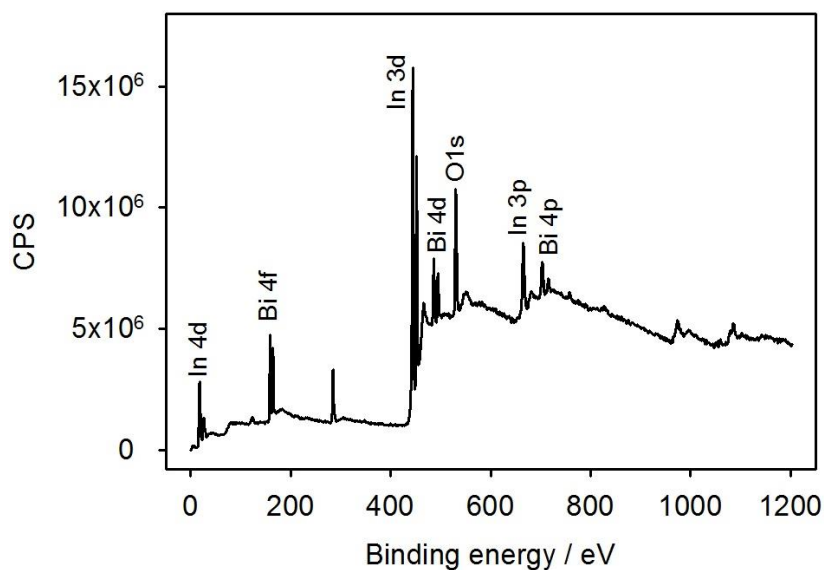


**Figure 5.** XPS of the prepared Bi@In hybrid nanofilm.

In order to verify the occurrence of Bi@In co-deposition on the electrode surface, XPS analysis was provided to calculate the elemental ratio of Bi to In within the Bi@In hybrid nanofilm. Either Bi

or In was clearly detected in the Bi@In hybrid film with a Bi/In mass ratio of 1:1, slightly lower than their original ratio in the mixed deposition solution (Fig. 5). This means that the co-deposition of bimetallic Bi@In actually occurred according to such a mass ratio.

### 3.3 Optimization of experimental conditions

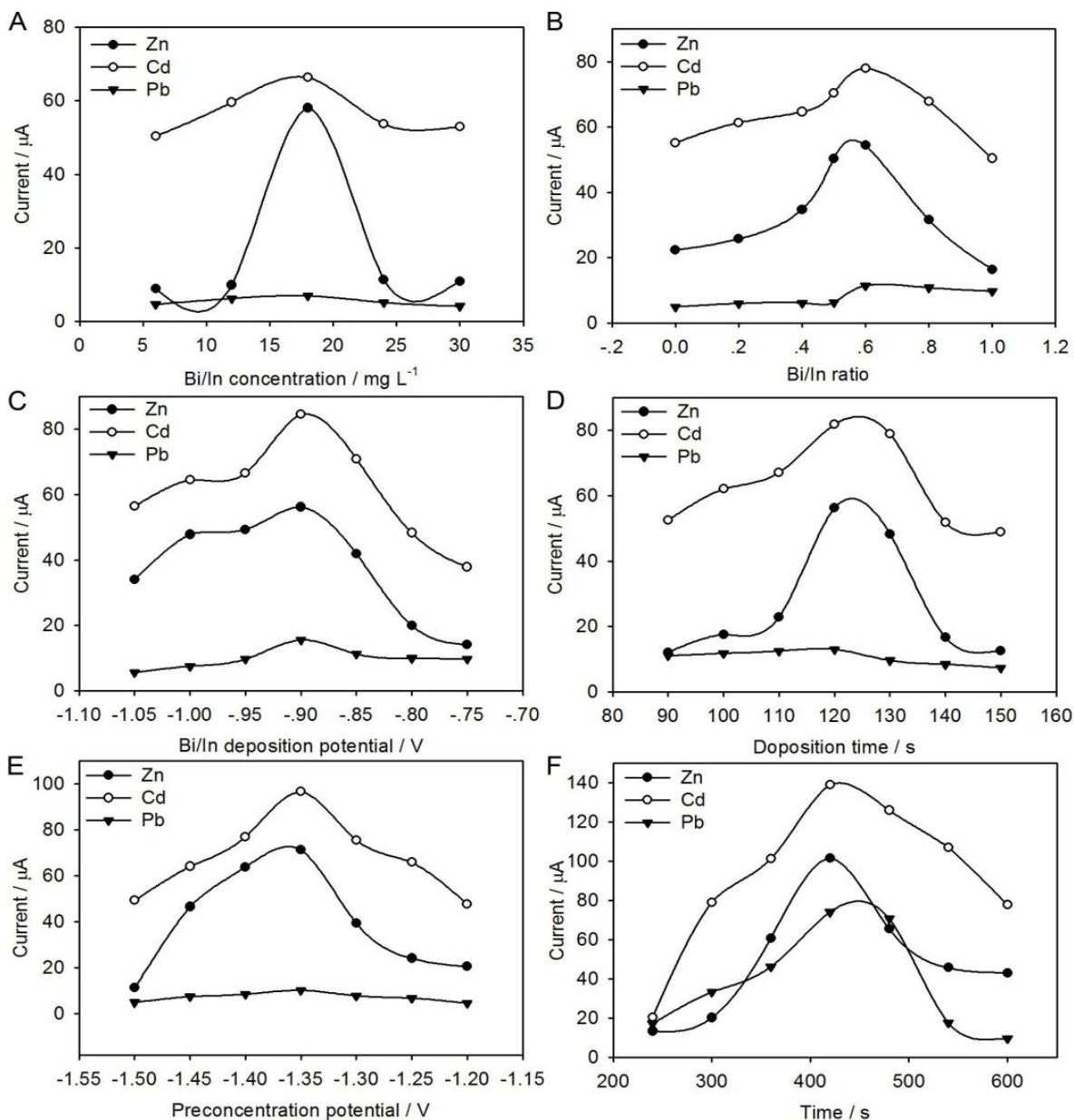


**Figure 6.** Effect of (A) the concentration of Bi(III) and In(III), (B) the mass ratio of Bi(III) to the sum of Bi(III) and In(III), (C and D) the co-deposition potential and time of Bi(III)/In(III) as well as (E and F) the preconcentration potential and time of Zn(II), Cd(II) and Pb(II) on the stripping signal of 100 µg L<sup>-1</sup> Zn(II), Cd(II) and Pb(II) in 0.1 M NaAc/HAc solution (pH 6.0). The experimental parameters for (A) were as follows: Bi(III)/In(III) ratio: 6:4; co-deposition potential: -0.95 V; co-deposition time: 120 s, preconcentration potential: -1.35V, preconcentration time: 360 s. The optimal parameter was selected after each optimization.

Several parameters were optimized in details so as to obtain the best response signal of Bi@In/GCE toward three metals, including the concentrations of Bi(III)/In(III) ions, the mass ratio of Bi(III) to In(III), the deposition potential and time of Bi(III)/In(III) as well as the preconcentration potential and time of Zn(II), Cd(II) and Pb(II) (Fig. 6).

### 3.3.1. Effect of Bi(III)/In(III) ion concentrations

The concentration of Bi(III)/In(III) ions partly controlled the particle size of the Bi@In hybrid, which significantly affected the electrochemical behavior of the prepared electrode[6]. As seen in Fig. 6A, the peak heights of Zn(II) and Cd(II) displayed clear dependence on Bi(III)/In(III) ion concentrations, but no obvious dependence was observed for Pb(II) peak signal. When the concentration of Bi(III)/In(III) ions was less than  $18 \text{ mg L}^{-1}$ , the peak height increased with the increasing Bi(III)/In(III) ion concentrations. Once more Bi(III)/In(III) ions was available, more Bi@In hybrid particles were produced with more active sites exposed to three metals. Whereas, the peak current decreased at Bi(III)/In(III) ion concentration higher than  $18 \text{ mg L}^{-1}$ . Since Bi@In hybrid particles grew bigger and bigger when more and more Bi(III)/In(III) ions were reduced, the negative effect on the electron transfer could accordingly result from a rough electrode surface. This might explain well why the stripping peaks decreased at Bi(III)/In(III) ion concentrations higher than  $18 \text{ mg L}^{-1}$ . Therefore,  $18 \text{ mg L}^{-1}$  Bi(III)/In(III) mixed solution were used to prepare Bi@In hybrid modified electrode

### 3.3.2 Effect of the mass ratio of Bi(III) to the sum of Bi(III) and In(III)

The synergistic effect of Bi and In in the bimetallic film was greatly influenced by the mass ratio of Bi(III), having a large impact on the activity enhancement of Bi@In/GCE. Fig. 6B shows the difference in detection performance of the Bi@In/GCE prepared at the different mass ratios of Bi(III) to the sum of Bi(III) and In(III). The peak current of Zn(II), Cd(II) and Pb(II) increased with the increasing ratio and reached the highest level at Bi(III)/Bi(III)+In(III) ratio of 3:5 (Bi(III)/In(III)=6:4). The peak current decreased with continuous increase in the Bi(III)/In(III) ratio. It means either lower or higher Bi(III)/In(III) ratio than 6:4 decreased the response to three metals, indicating the formation of Bi@In hybrid nanoparticles was considerably affected by the mass ratio of Bi(III)/In(III) ions in the mixed solution. The Bi@In hybrid films prepared at various Bi(III)/In(III) ratios led to different synergistic effect on the stripping signal of Bi@In/GCE toward Zn(II), Cd(II) and Pb(II). The results were in good agreement with that shown in Fig. 1 that both single Bi and In film modified electrodes exhibited poorer stripping signal toward Zn(II), Cd(II) and Pb(II) without synergistic effect. Therefore, the Bi(III)/In(III) ratio of 6:4 was selected for the subsequent assays.

### 3.3.3 Deposition potential and time of Bi(III) and In(III)

The stripping responses of Bi@In/GCE to Zn(II), Cd(II) and Pb(II) was also significantly affected by the deposition potential and time of Bi and In. The effect of the deposition potential on the

stripping signal was first explored in a potential range from -0.75 to -1.05 V (Fig. 6C). Bi@In/GCE showed higher and higher stripping signal toward three metals at more negative potentials and reached a maximum at -0.90 V and then gradually decreased when potentials more negative than -0.90 V were applied for the co-deposition. This was likely caused by the incomplete reduction of Bi and In at a more positive potential and the reduction of hydrogen at a more negative potential[6], which resulted in a poor surface morphology Bi@In hybrid film and finally affected the stripping behavior of Bi@In/GCE toward Zn(II), Cd(II) and Pb(II).

At the deposition potential of -0.90 V, the relationship between the stripping signal of Bi@In/GCE and the co-deposition time of Bi and In was subsequently studied between 90 s and 150 s (Fig. 6D). The peak heights increased proportionally with time before 125 s for both Zn(II) and Cd(II) and decreased afterwards. No obvious change was observed for Pb(II) at different deposition periods. Longer deposition time led to the formation of larger Bi@In nanoparticles which expose more active sites to target metals, while the electron transfer was inevitably blocked if Bi@In nanoparticles grew too large on GCE surface and accordingly caused decrease in the response signal of Bi@In/GCE toward Zn(II), Cd(II) and Pb(II). Therefore, the deposition potential and time of -0.90 V and 125 s were selected for the preparation of Bi@In hybrid nanofilm.

#### 3.3.4. Preconcentration potential and time of Zn(II), Cd(II) and Pb(II)

Fig. 6E shows that the stripping behavior of Bi@In/GCE changed with the preconcentration potential of Zn(II), Cd(II) and Pb(II) from -1.2 to -1.5 V. The stripping signals for Zn(II) and Cd(II) gradually increased with more negative potential applied and stopped going higher at -1.35 V. Though the increasing trend in stripping signal for Pb(II) was not quite obvious, the highest current was also obtained when -1.35 V was applied for the accumulation. This was because more negative potential made more metal ions accumulated on Bi@In/GCE surface, leading to the stripping signal increase. On the contrary, when potentials more negative than -1.35 V were applied to preconcentrate three metals, the peak signal decreased. This was likely caused by the significant hydrogen reduction at such negative potential[6].

With the potential of -1.35 V applied for preconcentration, the effect of the accumulation time was tested in the range from 240 to 600 s (Fig. 6F). The peak current greatly increased with longer time set for preconcentration of Zn(II), Cd(II) and Pb(II) and reached the maximum at 420 s owing to the continuous accumulation of three metals on the electrode surface. When the time was longer than 420 s, the peak currents of Zn(II) and Cd(II) obviously decreased due to the saturation of the available active sites on electrode surface for accumulation. In this case, once all active sites on Bi@In/GCE were fully occupied, no more metal ions could be efficiently accumulated on the electrode surface. Though the peak current of Pb(II) kept increasing till 450 s, it was high enough at 420 s for Pb(II) stripping detection. Thus, the preconcentration potential and time were selected as -1.35 V and 420 s for the accumulation of Zn(II), Cd(II) and Pb(II) on Bi@In/GCE.

## 3.4 Electrochemical measurements

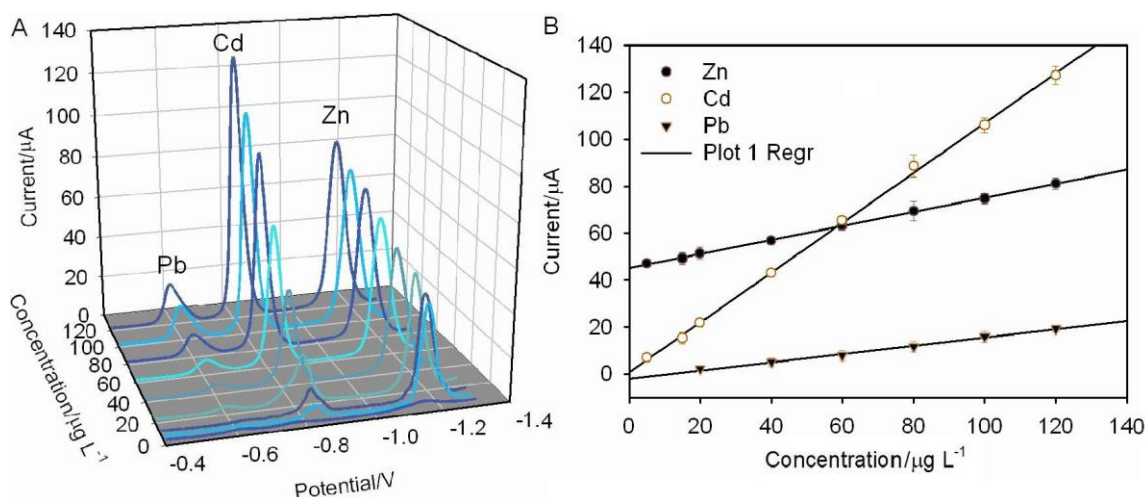


**Figure 7.** (A) Stripping performances and (B) corresponding calibration plots of Bi@In/GCE toward Zn(II), Cd(II) and Pb(II) at concentrations of 0, 5, 10, 20, 40, 60, 80, 100 and 120  $\mu\text{g L}^{-1}$ , respectively. Error bar:  $n=3$

**Table 1.** Comparison of the current sensor for the simultaneous stripping determination of Zn(II), Cd(II) and Pb(II) with some existing bismuth-based electrochemical sensors.

Electrodes	Linear range ( $\mu\text{g L}^{-1}$ )			Detection limit ( $\mu\text{g L}^{-1}$ )			Refs
	Zn(II)	Cd(II)	Pb(II)	Zn(II)	Cd(II)	Pb(II)	
NanoBiE	5-60	5-60	5-60	-	0.80	0.40	[5]
Bi-SPCE	75-200	0-70	0-70	54	0.69	0.89	[43]
Nafion/BiFE	0.65-6.5	1.1-11	2-20	1.6	0.66	0.60	[44]
Bi/CF/ME	0.033-0.65	0.06-1.1	-	0.052	$3.3 \times 10^{-3}$	-	[45]
Bi/Nafion/PANI-MES/GCE	-	0.10-20	0.10-30	-	0.04	0.05	[46]
Bi/Au-GN-Cys/GCE	-	0.50-40	0.50-40	-	0.1	0.05	[47]
Bi/poly(p-ABSA)	1-110	1-110	1-130	0.62	0.63	0.80	[48]
Bi/CNTs/SPCE	12-100	2-100	2-100	11	0.8	0.2	[49]
Hg-Bi/SWCNTs/GCE	10-130	10-130	10-130	2.0	0.98	1.3	[3]
Bi/Nafion/IL/GN/SPCE	0.1-100	0.1-100	0.1-100	0.09	0.06	0.08	[41]
$\text{Fe}_2\text{O}_3$ /GN/Bi	1-100	1-100	1-100	0.11	0.08	0.07	[42]
AgNP/Bi/Nafion/CSPEs	5.0-400	0.5-400	0.1-500	5.0	0.5	0.1	[50]
Bi@In/GCE	0-120	0-120	0-120	0.52	0.15	0.63	this work

Upon the optimization of parameters, the concentration range from 0 to 120  $\mu\text{g L}^{-1}$  was selected for the simultaneous stripping determination of Zn(II), Cd(II) and Pb(II) with Bi@In/GCE. As shown, three well-defined stripping signals of Zn(II), Cd(II) and Pb(II) were observed and the increase in peak current ( $i_p$ ) was in good proportion with the increasing concentrations of three metals (Fig. 7A). The calibration plot was well linear up to 120  $\mu\text{g L}^{-1}$  for each metal with linear regression equations of  $i_p =$

0.298C+45.2 for Zn(II),  $i_p= 1.06C+1.01$  for Cd (II) and  $i_p= 0.231C-1.79$  for Pb(II), respectively, where all correlation coefficients were higher than 0.995. Based on a signal-to-noise ratio equal to 3 (S/N = 3), the detection limits were calculated to be 0.52, 0.15 and 0.67  $\mu\text{g L}^{-1}$  for Zn(II), Cd (II) and Pb(II), respectively, comparable with some previous reports involving in bismuth-based electrodes (Table 1).

The sensitivities of 4218  $\mu\text{A} (\mu\text{g L}^{-1})^{-1} \text{cm}^{-2}$  for Zn(II), 1.5 mA  $(\mu\text{g L}^{-1})^{-1} \text{cm}^{-2}$  for Cd(II) and 3270  $\mu\text{A} (\mu\text{g L}^{-1})^{-1} \text{cm}^{-2}$  for Pb(II) were high enough for the determination of three metals in trace level. Though, with the combination of graphene and ionic liquid[41] or magnetic material  $\text{Fe}_2\text{O}_3$ [42] with Bi, the detection limits of three metals became better, there was no any obvious advantage over Bi@In/GCE in the linear range and their preparations were more complicated. Moreover, the detection limit with Bi@In/GCE was low enough for the detection of Zn(II), Cd(II) and Pb(II) in real samples. Such extraordinary stripping performance of Bi@In/GCE toward Zn(II), Cd(II) and Pb(II) was most likely attributed to the synergistic effect of the Bi@In hybrid nanocoating. All the obtained results indicate that a highly effective and efficient platform was constructed with Bi@In/GCE for Zn(II), Cd(II) and Pb(II) sensing and expected to be applied to real sample analysis.

### 3.5 Interference studies

**Table 2.** Interference study on the determination of Zn(II), Cd(II) and Pb(II) with the proposed Bi@In/GCE.

Foreign ions	$i_p^{\text{Zn}}$ decrease (%)	$i_p^{\text{Cd}}$ decrease (%)	$i_p^{\text{Pb}}$ decrease (%)
$\text{Nd}^{3+}$	27.31	4.69	5.72
$\text{Y}^{3+}$	8.72	5.64	2.37
$\text{Ni}^{2+}$	32.83	12.37	9.28
$\text{Ce}^{3+}$	-5.72	4.98	-1.27
$\text{Fe}^{3+}$	4.67	-7.92	3.78
$\text{Co}^{2+}$	14.76	12.89	8.92
$\text{Sb}^{3+}$	-6.87	9.27	7.93
$\text{Cs}^+$	2.78	-5.12	3.24
$\text{Mg}^{2+}$	3.56	6.43	-1.28
$\text{SO}_4^{2-}$	3.14	-1.24	4.76
$\text{NO}_3^-$	6.79	-11.27	-5.78

Before using the electrodes for real environmental sample analysis, the effects of potentially interfering metals present in river water were investigated. Since in the presence of some other co-existing ions, the active sites supposed to sense analyte ions on Bi@In/GCE surface were possibly occupied, which interfered with anodic stripping determination of 100  $\mu\text{g L}^{-1}$  Zn(II), Cd(II) and Pb(II).

Thus 11 foreign ions like  $\text{Nd}^{3+}$ ,  $\text{Y}^{3+}$ ,  $\text{Bi}^{3+}$ ,  $\text{SO}_4^{2-}$  etc. were selected to evaluate the potential interference with the simultaneous stripping detection of three metals, where the mass ratio of each foreign ion to target metals was 200 (Table 2). The peak current decrease was used for the interference investigation and the foreign ion was considered as interferent when it caused a current decrease by ca. 10% or higher of the initial response to the target metals. The results shown in Table 2 indicated that only Nd(III), Ni(II) and Co(II) caused the obvious influences in the signals of Zn(II) and Ni(II) and Co(II) were found to slightly suppress the signals of Cd(II). No obvious interferences were found for the detection of Pb(II) by all the tested interfering ions. The competition of the active sites between target metals and interfering ions and intermetallic compound formation on Bi@In/GCE might be the major factor causing the interferences[3]. The other 9 coexisting ions exhibited no interferences with determination of Zn(II), Cd(II) and Pb(II), revealing the excellent selectivity of the proposed Bi@In/GCE.

### 3.6 Reproducibility and stability

A relative standard deviation (RSD) lower than 3.0 % was achieved for anodic stripping determination of  $100 \mu\text{g L}^{-1}$  Zn(II), Cd(II) and Pb(II) within five independently prepared Bi@In/GCE, indicating a good fabrication reproducibility. The short- and long-term stabilities were additionally studied, where the short-term stability was assessed by continuously measuring  $100 \mu\text{g L}^{-1}$  Zn(II), Cd(II) and Pb(II) for 10 times using one as prepared Bi@In/GCE. For all three metals, the last measured peak currents decreased by 3.0% or lower in regards to the first measured ones, indicating a good short-term stability of the Bi@In hybrid based sensor. Therefore, the designed electrode could be continuously used for the repeated measurements without obvious decrease in stripping signal. In order to evaluate the performance of the sensor in a full-scale way, the long-term stability was investigated as well. The stripping signals of Bi@In/GCE toward  $100 \mu\text{g L}^{-1}$  Zn(II), Cd(II) and Pb(II) were recorded every other day. Four weeks later, the responses to three metals showed no less than 90% of their initial response signals, indicative of the good long-term stability. The synergistic effect of Bi@In hybrid was likely the major factor leading to such good reproducibility and stability of the sensor. All the results implied that the designed Bi@In/GCE was reproducible, stable and reliable for the simultaneous detection of Zn(II), Cd(II) and Pb(II) in aqueous solution.

### 3.7 Sample analysis

With the aim to verify the reliability of proposed novel Bi@In/GCE in the practical application, the river water samples were collected from Pujiang River in Shanghai (China) to measure the contents of Zn(II), Cd(II) and Pb(II) with Bi@In/GCE. Concentrations were validated using ICP-MS.

As seen in Fig. 8, three well-defined stripping signals in water sample was observed with the newly developed Bi@In/GCE. The original concentrations of Zn(II), Cd(II) and Pb(II) in the river samples were measured to be  $54.61 \pm 1.71$ ,  $0.76 \pm 0.03$  and  $2.07 \pm 0.07 \mu\text{g L}^{-1}$ , respectively (Table 3). The

accuracy of the new method was estimated by the standard additions of 10 and 20  $\mu\text{g L}^{-1}$  in river water and data comparison with ICP-MS.

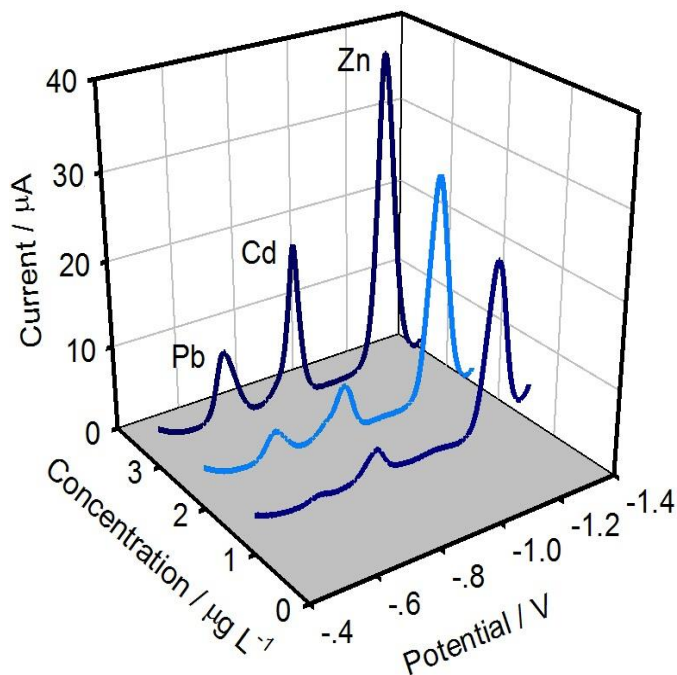


**Figure 8.** Stripping performances of Bi@In/GCE toward Zn(II), Cd(II) and Pb(II) in river samples added with 0, 10 and 20  $\mu\text{g L}^{-1}$  of three standard metals, respectively.

**Table 3.** Determination of Zn(II), Cd(II) and Pb(II) in the collected river water samples with Bi@In/GCE and ICP-MS.

	Added ( $\mu\text{g L}^{-1}$ )	Founded by ICP- MS ( $\mu\text{g L}^{-1}$ )	Founded by new method ( $\mu\text{g L}^{-1}$ ) <sup>a</sup>	Recovery (%)
Zn(II)	-	53.67±1.6	54.61±1.7	-
	10	63.96±2.2	64.21±2.0	106
	20	79.34±2.0	76.01±1.9	107
Cd(II)	-	0.72±0.04	0.76±0.03	-
	10	10.74±0.38	10.96±0.32	102
	20	19.80±0.79	20.51±0.61	98.7
Pb(II)	-	1.98±0.10	2.07±0.07	-
	10	12.03±0.50	12.05±0.48	99.8
	20	22.32±0.60	22.67±0.56	103

<sup>a</sup> Each measurement was performed for 3 times.

Good recoveries over 98% were obtained and the measurement results were in good accordance with that from ICP-MS. Also RSDs lower than 5.0 % (n=3) for Zn(II), Cd(II) and Pb(II) measurements were achieved. It was, therefore, concluded that the proposed method was accurate, precise, reproducible and potentially used as a preferable alternative for direct analysis of Zn(II), Cd(II) and Pb(II) in other real samples.

#### 4. CONCLUSION

A highly effective and sensitive platform for the stripping analysis of Zn(II), Cd(II) and Pb(II) was successfully developed based on a Bi@In hybrid nanofilm on GCE. The presence of In or Bi was proved to significantly enhance each other's stripping performance toward three metals in the bimetallic form of Bi@In. The synergistic effect of Bi@In hybrid made major contributions to such excellent stripping performance of Bi@In/GCE by improving its surface morphology, electron transfer rate as well as hydrophilicity. The practical application of in river water provided evidence that the newly fabricated Bi@In hybrid based sensor was sensitive, selective, accurate and reliable in the stripping determination of Zn(II), Cd(II) and Pb(II) and considered as an attractive replacement of other existing sensor.

#### ACKNOWLEDGEMENTS

This work was supported by the State Key Laboratory of Analytical Chemistry for Life Science (SKLACLS1502), the National Natural Science Foundation of China (21305090), the Innovation Program of Shanghai Municipal Education Commission (14YZ086). The authors greatly appreciated these supports.

#### References

1. S. Chaiyo, E. Mehmeti, K. Žagar, W. Siangproh, O. Chailapakul, K. Kalcher, *Anal. Chim. Acta*, 918 (2016)26.
2. N. Ruecha, N. Rodthongkum, D.M. Cate, J. Volckens, O. Chailapakul, C.S. Henry, *Anal. Chim. Acta*, 874 (2015)40.
3. R.Z. Ouyang, Z.Q. Zhu, C.E. Tatum, J.Q. Chambers, Z.L. Xue, *J. Electroanal. Chem.*, 656 (2011)78.
4. M.Á.G. Rico, M. Olivares-Marín, E.P. Gil, *Talanta*, 80 (2009)631.
5. D. Yang, L. Wang, Z. Chen, M. Megharaj, R. Naidu, *Microchim. Acta*, 181 (2014)1199.
6. L.N. Xu, R.Z. Ouyang, S. Zhou, H.F. Wen, X. Zhang, Y. Yang, N. Guo, W.W. Li, X. Hu, Z.Y. Yang, L. Ouyang, Y.Q. Miao, *J. Electrochem. Soc.*, 161 (2014)H730.
7. R.Z. Ouyang, W.Y. Zhang, S.L. Zhou, Z.L. Xue, L.N. Xu, Y.Y. Gu, Y.Q. Miao, *Electrochim. Acta*, 113 (2013)686.
8. R.Z. Ouyang, S.A. Bragg, J.Q. Chambers, Z.L. Xue, *Anal. Chim. Acta*, 722 (2012)1.
9. D. Wilson, J.M. Gutierrez, S. Alegret, M. del Valle, *Electroanal.*, 24 (2012)2249.
10. M.A.G. Rico, M. Olivares-Marin, E.P. Gil, *Electroanal.*, 20 (2008)2608.

11. J. Kudr, H. Nguyen, J. Gumulec, L. Nejd, I. Blazkova, B. Ruttkay-Nedecky, D. Hynek, J. Kynicky, V. Adam, R. Kizek, *Sensors*, 15 (2015)592.
12. S. Muralikrishna, D.H. Nagaraju, R.G. Balakrishna, W. Surareungchai, T. Ramakrishnappa, A.B. Shivanandareddy, *Analytica chimica acta*, 990 (2017)67.
13. Y.F. Zhao, L.B. Xu, M. Liu, Z.Q. Duan, H. Wang, *Food Chem.*, 239 (2018)40.
14. M. Tuzen, S. Sahiner, B. Hazer, *Food. Chem.*, 210 (2016)115.
15. T. Dasbasi, S. Sacmaci, A. Ulgen, S. Kartal, *Food. Chem.*, 197 (2016)107.
16. K. Jusufi, T. Stafilov, M. Vasjari, B. Korca, J. Halili, A. Berisha, *Fresenius Environ. Bull.*, 25 (2016)1313.
17. G.L. Peng, Y. Lu, Q. He, D. Mmereki, G.M. Zhou, J.H. Chen, X.H. Tang, *J. AOAC Int.*, 99 (2016)260.
18. N. Thinakaran, E. Subramani, T. Priya, N. Dhanalakshmi, T.V. Vineesh, V. Kathikeyan, *Electroanalysis*, 29 (2017)1903.
19. D. Martin-Yerga, I. Alvarez-Martos, M.C. Blanco-Lopez, C.S. Henry, M.T. Fernandez-Abedul, *Analytica chimica acta*, 981 (2017)24.
20. Q.X. Zhang, H. Wen, D. Peng, Q. Fu, X.J. Huang, *J. Electroanal. Chem.*, 739 (2015)89.
21. K.C. Armstrong, C.E. Tatum, R.N. Dansby-Sparks, J.Q. Chambers, Z.L. Xue, *Talanta*, 82 (2010)675.
22. Z. Guo, W. Hui, Y. Yuan, L. Gang, *Int. J. Agric. Biol. Eng.*, 10 (2017)251.
23. G.J. Lee, C.K. Kim, M.K. Lee, C.K. Rhee, *J. Electrochem. Soc.*, 157 (2010)J241.
24. H.X. Guo, Z.S. Zheng, Y.H. Zhang, H.B. Lin, Q.B. Xu, *Sens. Actuator B-Chem.*, 248 (2017)430.
25. X.L. Zhu, B.C. Liu, H.J. Hou, Z.Y. Huang, K.M. Zeinu, L. Huang, X.Q. Yuan, D.B. Guo, J.P. Hu, J.K. Yang, *Electrochim. Acta*, 248 (2017)46.
26. S.B. Khoo, S.X. Guo, *Electroanal.*, 14 (2002)813.
27. E. Munoz, S. Palmero, M.A. Garcia-Garcia, *Talanta*, 57 (2002)985.
28. B.S. Sherigara, Y. Shivaraj, R.J. Mascarenhas, A.K. Satpati, *Electrochim. Acta*, 52 (2007)3137.
29. A. Babaei, E. Shams, A. Samadzadeh, *Anal. Sci.*, 22 (2006)955.
30. F. Shemirani, M. Rajabi, *J. Anal. Chem.*, 62 (2007)878.
31. J. Wang, J.M. Lu, S.B. Hocevar, P.A.M. Farias, B. Ogorevc, *Anal. Chem.*, 72 (2000)3218.
32. A. Economou, A. Voulgaropoulos, *Electroanal.*, 22 (2010)1468.
33. G.M.S. Alves, J. Magalhaes, H. Soares, *Electroanal.*, 23 (2011)1410.
34. L. Zhu, L.L. Xu, B.Z. Huang, N.M. Jia, L. Tan, S.Z. Yao, *Electrochim. Acta*, 115 (2014)471.
35. S. Dal Borgo, H. Sopha, S. Smarzewska, S.B. Hocevar, I. Svancara, R. Metelka, *Electroanal.*, 27 (2015)209.
36. C.L. Jost, L.M. di Martos, L. Ferraz, P.C. do Nascimento, *Electroanal.*, 28 (2016)287.
37. Y.X. Tao, X.G. Gu, Y. Pan, L.H. Deng, Y. Wei, Y. Kong, W. Li, *J. Electrochem. Soc.*, 162 (2015)H194.
38. L. Baldrianova, P. Agrafiotou, I. Svancara, A.D. Jannakoudakis, S. Sotiropoulos, *J. Electroanal. Chem.*, 660 (2011)31.
39. M. Slavec, S.B. Hocevar, B. Ogorevc, *Electroanal.*, 20 (2008)1309.
40. X. Hu, Y.Q. Miao, S.L. Zhou, X.C. Liang, *J. Nanosci. Nanotechnol.*, 15 (2015)628.
41. S. Chaiyo, E. Mehmeti, K. Zagar, W. Siangproh, O. Chailapakul, K. Kalcher, *Analytica chimica acta*, 918 (2016)26.
42. S. Lee, J. Oh, D. Kim, Y. Piao, *Talanta*, 160 (2016)528.
43. S. chuanwatanakul, W. Dungchai, O. Chailapakul, S. Motomizu, *Anal. Sci.*, 24 (2008)589.
44. V. Rehacek, I. Hotovy, M. Vojs, T. Kups, L. Spiess, *Electrochim. Acta*, 63 (2012)192.
45. A.P.R. de Souza, M.O. Salles, E.S. Braga, M. Bertotti, *Electroanal.*, 23 (2011)2511.
46. L. Chen, Z. Su, X. He, Y. Liu, C. Qin, Y. Zhou, Z. Li, L. Wang, Q. Xie, S. Yao, *Electrochem. Commun.*, 15 (2012)34.
47. L. Zhu, L. Xu, B. Huang, N. Jia, L. Tan, S. Yao, *Electrochim. Acta*, 115 (2014)471.

48. Y. Wu, N.B. Li, H.Q. Luo, *Sens. Actuat. B-Chem.*, 133 (2008)677.
49. U. Injang, P. Noyrod, W. Siangproh, W. Dungchai, S. Motomizu, O. Chailapakul, *Anal. Chim. Acta*, 668 (2010)54.
50. J. Mettakoonpitak, J. Mehaffy, J. Volckens, C.S. Henry, *Electroanal.*, 29 (2017)880.

© 2018 The Authors. Published by ESG ([www.electrochemsci.org](http://www.electrochemsci.org)). This article is an open access article distributed under the terms and conditions of the Creative Commons Attribution license (<http://creativecommons.org/licenses/by/4.0/>).